Balancing Degradability and Physical Properties of Amorphous Poly(D,L-Lactide) by Making Blends

Anil Kumar, Alfons R. Weig, and Seema Agarwal*

The problem in using the existing biodegradable polymers for day-to-day commodity and specialty applications (non-physiological) is the trade-off between the degradability and physical properties of polymers. Therefore, the authors study the properties of polyester films made by solution blending of amorphous poly(D,L-lactide) and semi-crystalline poly(L,L-lactide) (PLLA) with an aim to achieve a good balance of mechanical properties and degradability under environmental conditions. The degradation test using proteinase K enzyme shows faster degradation of blends in comparison to homopolymers by weight loss. Faster fragmentation of blends and fragments of lower masses in comparison to PLLA is also seen in immature compost with bulk degradation as the main mechanism of degradation. A detailed investigation shows increased crystallinity and the formation of crystalline stereo-complex in fragmented samples that may limit degradation after a stage causing microplastics persisting for a longer period. Therefore, further degradation studies in compost for at least 8–10 weeks are recommended. Other environmental sinks, such as activated sludge water, fresh, and seawater, provide either extremely slow or no degradation excluding the use of such blends for applications intended for these sinks. In future, smart solutions are required to enhance the degradation of polylactide in different environmental sinks.

1. Introduction

Synthetic biodegradable polymers are attracting attention as one of the solutions for the problem of ever-increasing plastic

A. Kumar, S. Agarwal
Macromolecular Chemistry II
University of Bayreuth
Universitätsstraße 30, Bayreuth 95440, Germany
E-mail: agarwal@uni-bayreuth.de
A. R. Weig
Genomics and Bioinformatics
Bayreuth Center of Ecology
and Environmental Research (BayCEER)
University of Bayreuth
Universitätsstrasse 30, Bayreuth 95440, Germany

waste.[1,2] Although biodegradable polymers are not the only solution for plastic pollution, they can provide a sustainable solution, especially in applications where it is not easy to collect the polymers back after use.[3] Agricultural applications and food packaging are some of these important application areas. The current class of polymers being considered and studied as biodegradable polymers is aliphatic and aliphatic–aromatic polyesters. The ester functional groups in polymer backbone repeat units can be hydrolyzed under appropriate environments leading to the breakage of the polymer chain (fragmentation) followed by bio-assimilation of fragmented oligomers and monomers to carbon dioxide (CO_2), water, and biomass.[4–9] This two-step process is called biodegradation. The first step of biodegradation, the process of fragmentation to oligomers and monomers, is highly critical for the whole process of biodegradation as long macromolecule chains with high molar mass cannot be bio-assimilated.

Crystallinity is one of the important factors affecting the rate of fragmentation by hydrolysis of polyesters.[10] The amorphous polyesters are fast-hydrolyzable in comparison to the semi-crystalline ones as shown for the hydrolysis of poly(D,L-lactide) (PDLLA), a racemic and amorphous counterpart of isotactic, semi-crystalline poly(L,L-lactide) (PLLA) in phosphate-buffered solution (PBS) of pH 7.4 at 37 °C.[11,12] This is true for enzymatic hydrolysis also, as the polylactide with higher content of *L*-units is slowly hydrolyzable during enzymatic hydrolysis.[10]

The problem in using the existing biodegradable polymers for day-to-day commodity and specialty applications (non-physiological) is the trade-off between the degradability and physical properties of polymers. For example, amorphous polyester like PDLLA is fast-degradable but shows poor mechanical properties and use low temperature due to its low glass transition temperature ($T_g \approx 60$ °C). Another example is an amorphous copolymer of *L*-lactide and glycolide (PLGA) which shows significant degradation even in the sea and freshwater but has a very low T_g of ≈35–40 °C limiting its use.[13]

Recently, we showed faster degradation with good mechanical properties of layer-by-layer films of PLLA in which PLLA thin layers were separated with layered silicates.[14] Blending commercially available polymers for property tuning is the most straightforward method. For example, amorphous PDLLA was blended

ADVANCED SCIENCE NEWS
www.advancedsciencenews.com

Macro-
molecular
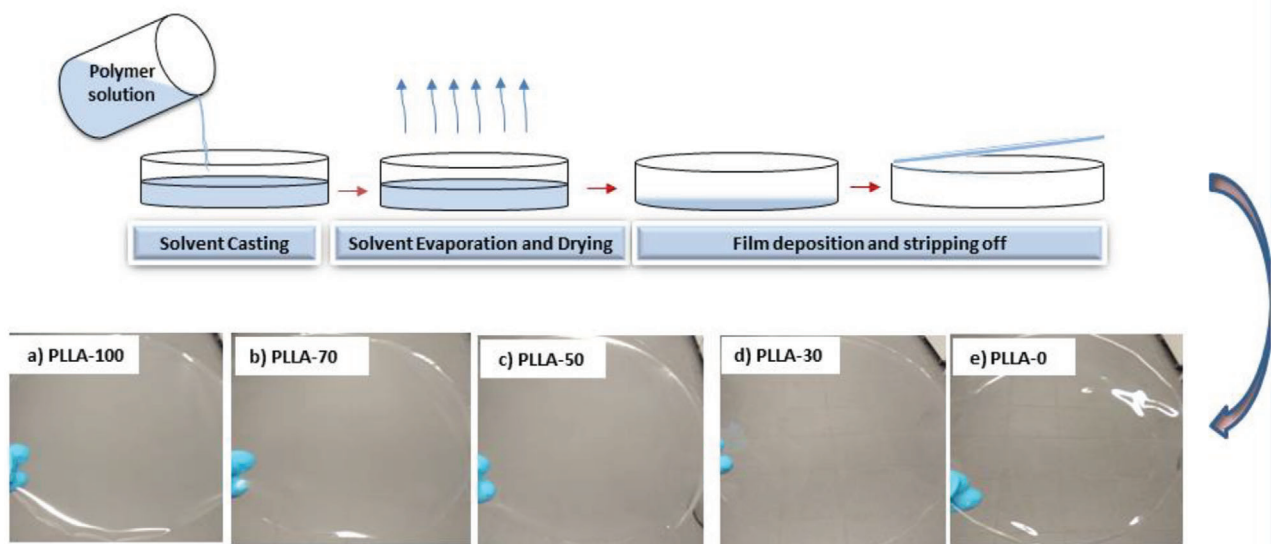**Materials** and **Engineering**
www.mame-journal.de

Figure 1. Solution cast films of semi-crystalline PLLA and its blends with amorphous PDLLA in chloroform. The diameter of the films was ≈15 cm. a) to e) are the blend films with different ratios of PDLLA and PLLA.

with semi-crystalline polycaprolactone,[15,16] and polyglycolide in order to study the effect on the physical properties and hydrolyzability in PBS buffer.[15,17] The blend of PDLLA with the isotactic polylactide (PLLA) was also studied and showed interestingly that PDLLA does not hinder the crystallization of PLLA beyond a critical amount of PLLA in the blend.[18] Also, below a critical ratio of PLLA:PDLLA, the similar hydrolyzability of blends as that of PDLLA in PBS buffer could be achieved.[11] Therefore, this blend system might be interesting for balancing the mechanical properties and fragmentation by hydrolyzability (the first step of biodegradation) and final biodegradability under controlled and uncontrolled environmental conditions by choosing the appropriate ratio of PDLLA and PLLA in blends.

Motivated with this, we carried out a basic study and present here our recent results regarding solution blending of the amorphous PDLLA and semi-crystalline PLLA in different ratios, their crystallization behavior before and after degradation, mechanical characteristics, and fragmentation behavior under enzyme and environmental conditions in compost, waste-water, fresh and artificial seawater. The change in morphology, crystallinity, molar mass, and formation of stereo-complex between the *L*- and *D*-rich fragments formed during degradation led to the detailed understanding of the degradation mechanism.

2. Results and Discussion

Blending of semi-crystalline PLLA (Molecular weight, M_n = 118 000 g mol^{-1}, *D*-content = 4.3%) and amorphous PDLLA (Molecular weight, M_n = 112 000 g mol^{-1}, *D*-content = 12%) was carried out in chloroform using 100:0, 70:30, 50:50, 30:70, and 0:100 weight ratio of the PLLA and PDLLA, respectively. We designated blends as PLLA-*X*, where *X* is the wt% of PLLA in the blend. Based on this designation, the PLLA-0 means amorphous PDLLA. The homopolymer and the blend films obtained

are shown with a schematic diagram of the solvent casting approach (**Figure 1**).

The optical properties of films were measured using UV/vis spectrophotometer by measuring transmission at 650 nm (Figure S1, Supporting Information). The blend films with increased amounts of PDLLA were optically more transparent than the homopolymer PLLA film. In **Figure 2**a, XRD patterns showed the semi-crystalline nature of all blends with prominent crystalline peaks of PLLA at $2\theta \approx 16.8°$ and 19.5°, which corresponds to the reflection planes (110) and (203), respectively.[19] This shows that PDLLA did not hinder the crystallization of PLLA. Further semi-crystalline nature of all blends was confirmed by the differential scanning calorimetric (DSC) measurements (Figure 2b and Table S1, Supporting Information), showing a melting peak at 148 ± 2 °C with no significant change in the melting temperature with blend composition. Additionally, two separate glass transitions were obvious in samples PLLA-30 and PLLA-70 for semi-crystalline PLLA and amorphous PDLLA, showing phase-separated morphology. A decrease in the melting enthalpy and overall crystallinity of the blends was obtained with decreasing amount of semi-crystalline PLLA in the blends. Crystallinity was calculated based on the theoretical value of 93 J g^{-1} for 100% crystalline PLLA.[20] The PLLA could crystallize faster in the presence of the amorphous PDLLA in blends, as evident from normalizing the melting enthalpy to the actual weight of PLLA in blends. The normalized % crystallization values for PLLA increased on increasing the amount of more mobile amorphous PDLLA phase (Table S1, Supporting Information). This is beneficial as it overcomes slow crystallization tendency, one of the limitations of pure PLLA.

The semi-crystalline nature of blends was also observed under the polarized light microscope (Figure S2, Supporting Information). The PLLA-100 film showed bigger spherulites. The spherulite size decreased with the increased amount of amorphous PDLLA. For PLLA-30 with the least amount of PLA in
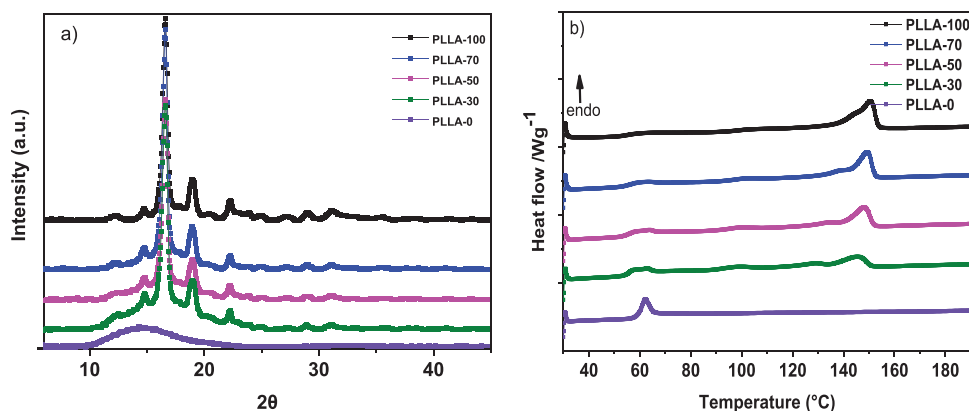
**ADVANCED
SCIENCE NEWS**

www.advancedsciencenews.com

**M acro-
olecular
Materials and Engineering**

www.mame-journal.de

Figure 2. a) XRD patterns, and b) DSC first heating curves of blends of semi-crystalline PLLA with amorphous PDLLA.
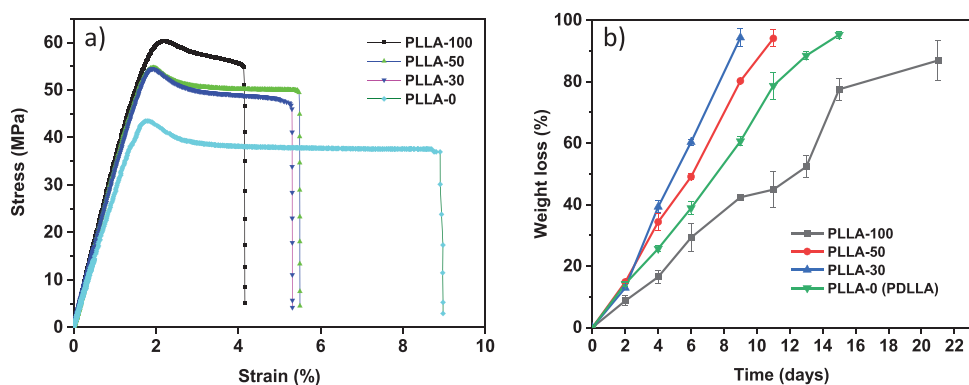

Figure 3. a) Stress and strain curves, and b) proteinase-K mediated degradation as monitored by weight loss of PLLA-100 and PLLA-0 and their blends.

blends studied in the present work, PDLLA dark continuous domains surround all over the PLLA small crystallites.

All blends were thermally stable at least till more than 320 °C as studied by thermogravimetric analysis (TGA) (Figure S3, Supporting Information). The blend films were strong, showed the tensile strength and the elongation at a break between the two homopolymers, PLLA (55 MPa) and PDLLA (37 MPa) (**Figure 3**a).

Further, the effect of blending on the degradability was considered under controlled laboratory conditions using Proteinase-K at 37 °C in Tris buffer by following the mass loss with time (Figure 3b).[21] The physical observation of the samples after different degradation times showed intact films (Figure S4, Supporting Information) but reduced in thickness. After 6/9 days of degradation, depending upon the composition, the films started breaking in the degradation medium. The pH of the enzymatic medium was measured every 24 h before changing the buffer/enzyme fresh solution. The pH of media was slightly decreased from 8.6 to 8.2 within 24 h. The evidence of pH decreasing was also reported in the literature for the degradation of pure PLLA to the formation of carboxyl (–COOH) and hydroxyl group (–OH) containing intermediate degradation products.[22] In fact, the carboxyl acid and hydroxyl functional degradation intermediates are very obvious from the backbone structure of the polymers also. The order of enzymatic degradation observed is: PLLA-30 > PLLA-50 > PLLA-0 > PLLA-100. Interestingly, the enzyme-catalyzed hydrolysis of the ester units in PLLA blends enhanced

in comparison to the semi-crystalline PLLA. This can be attributed to the overall reduced crystallinity of blends in comparison to that of PLLA. Further noteworthy is that the semi-crystalline blends degraded faster than the amorphous PDLLA. If crystallinity is the only reason affecting enzymatic degradation, then PDLLA without any crystallinity should have been degrading the fastest. To get insight into the degradation behavior the change in molar mass of homopolymers and their blends were studied by gel permeation chromatography (GPC) (**Figure 4**). It was obvious from GPC measurement of the undegraded rest that despite the weight loss as seen by gravimetry, the high molar mass main peak ($M_p \approx 1.55 \times 10^5$) was not affected by the degradation for the PLLA-0 (PDLLA). In addition, some low molar mass fractions were obvious in the low molar mass region. No significant shift in the high molar mass peak is an indication of degradation by surface erosion. Also, the presence of very low molar mass species in GPC hints at restricted mass transport of the degraded species in the degrading medium. On the other hand, the PLLA and its blends showed, in the beginning, a slight shift of the main high molar mass peak ($M_p \approx 2.0 \times 10^5$, 1.97×10^5, and 1.99×10^5 for PLLA-100, PLLA-50, and PLLA-30, respectively) to low molar mass ($M_p \approx 1.14 \times 10^5$, 1.23×10^5, and 1.45×10^5 for PLLA-100, PLLA-50, and PLLA-30, respectively), and afterward remained the same as degradation progressed. This implies a heterogeneous degradation mechanism (both bulk and surface erosion dominated by bulk in the beginning),
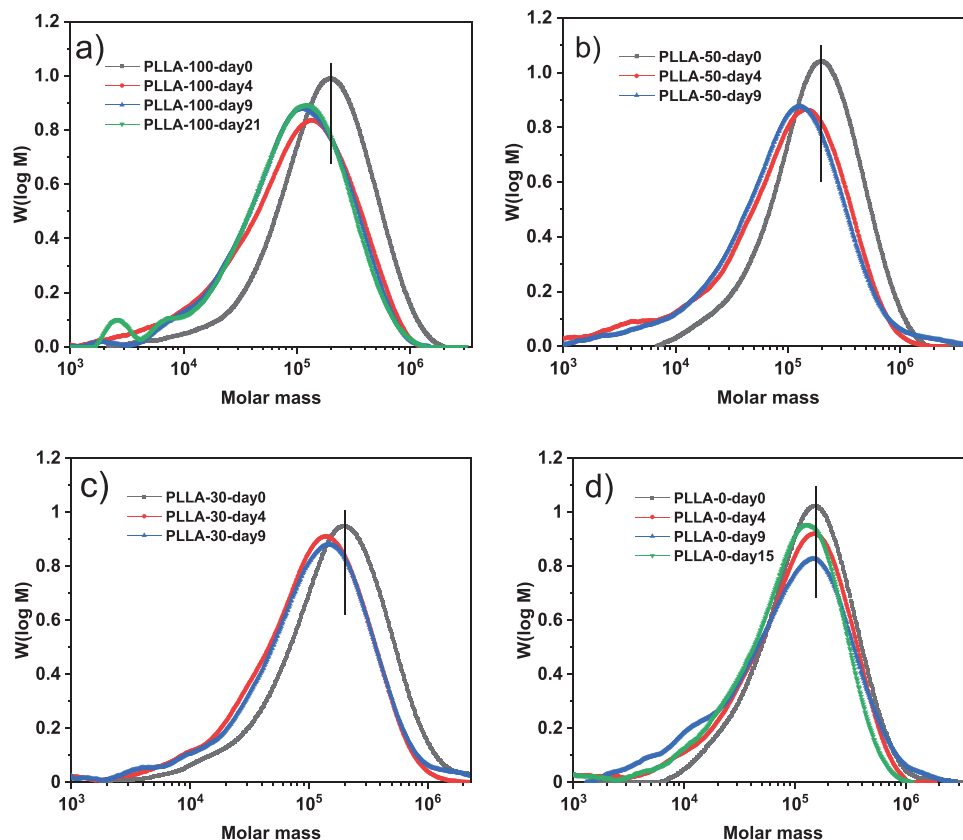
ADVANCED
SCIENCE NEWS
www.advancedsciencenews.com

[M] **acro-**
olecular
Materials and **Engineering**
www.mame-journal.de

Figure 4. Molar mass distribution curves as determined by CHCl$_3$-gel permeation chromatography (GPC) of a) PLLA-100, b) PLLA-50, c) PLLA-30, and d) PLLA-0 before and during enzymatic degradation at different time intervals.
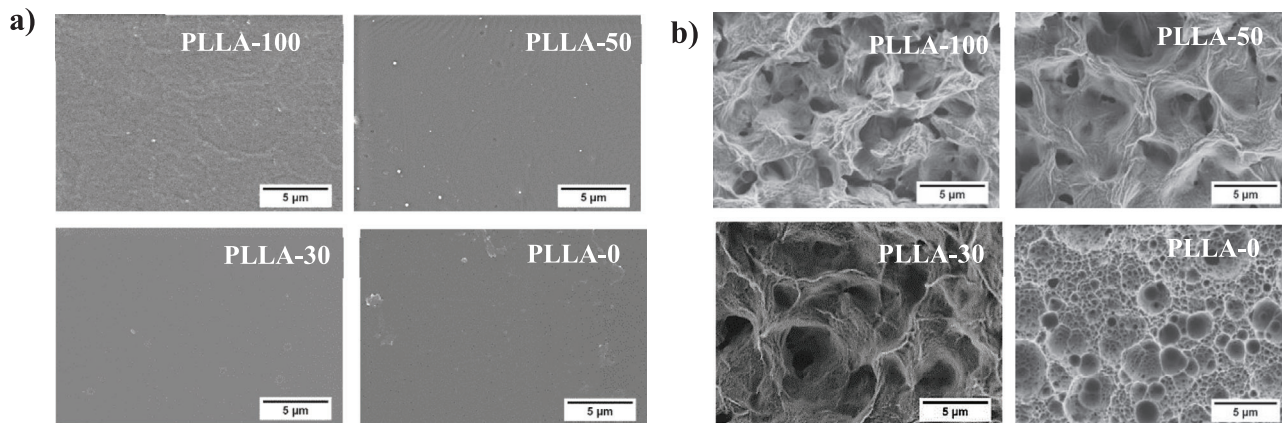

Figure 5. Scanning electron microscope (SEM) images of PLLA and its blends with PDLLA a) before and b) after degradation by Proteinase K enzyme.

providing a faster mass loss and explaining the faster degradation of blends compared to the amorphous PDLLA.

The surface characterization by scanning electron microscopy (SEM) of the samples before and after degradation also confirmed surface erosion as the main degradation mechanism. **Figure 5** shows SEM images; the surface of the blend samples after degradation showed the formation of a dual porous structure with large closed pores and small open pores of several

micrometers. PDLLA, after degradation, showed several smaller pores than blends. This contrasts with the smooth surfaces before degradation.

After screening test under controlled laboratory conditions, we tested degradation of films in fresh compost, which was ≈4 weeks old at 58 ± 2 °C and humidity 55–60%, that is, test conditions as specified by ASTM D5338. The test was run specifically for 40 days, and after this, visible undegraded film fractions
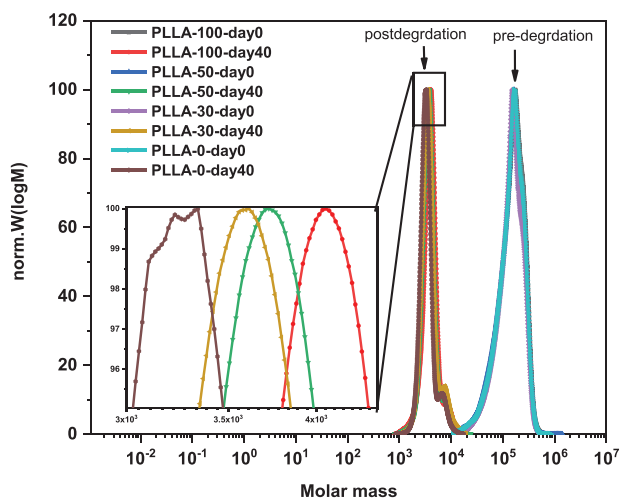
**ADVANCED
SCIENCE NEWS**
www.advancedsciencenews.com

acro-
olecular
Materials and **Engineering**
www.mame-journal.de

Figure 6. HFIP-gel permeation chromatography (GPC) curves of PLLA and its blends before and after 40 days of degradation in compost.

(Figure S5, Supporting Information) were isolated from the compost, washed with water, dried for 48 h, and then analyzed further. The undegraded samples were very brittle and broke when touched. It was not possible to conclude the degradability trend among various samples by mass balance as undegraded samples could not be manually collected with 100% precision from the compost. We tried to be as precise as possible in the manual collection of the undegraded samples after 40 days and observed from the mass loss that the highest degradation was observed for amorphous PLLA-0 (PDLLA) (54 wt%), followed by PLLA-30 (40 wt%), PLLA-50 (32 wt%), and PLLA-100 (23 wt%). This trend follows the increasing crystallinity trend: PLLA100 > PLLA-50 > PLLA-30 > PLLA-0 (PDLLA). Further, the isolated film samples were analyzed by GPC for studying the change in molar mass, if any. Some important conclusions could be made based on the GPC curves (**Figure 6**). First, there was a very significant decrease in the molar mass of all samples, with the appearance of new low molar mass fragments indicating degradability of the samples in compost by bulk degradation process. Second, the molar mass of the remaining fragments decreased with the decrease in the amount of PLLA in blends (Figure 6, inset).

Further, from the DSC analysis of the undegraded samples, three important observations were made. These observations are a significant decrease in the melting point, an increase in the crystallinity of the samples (melting enthalpy increased), and crystallization of pristine amorphous sample, PLLA-0 (**Figure 7**). The decrease in the melting point and increase in the crystallinity of pristine semi-crystalline PLLA is actually no surprise, as this is in agreement with the reported results for PLLA hydrolysis in PBS buffer.[23] An increase in crystallinity of PLLA during alkaline hydrolysis was also observed.[24] The degradation of PLLA in compost by hydrolysis of the ester linkages starts in the amorphous region, thereby increasing the crystallinity in undegraded fragments. Also, the increased mobility of chains in degraded fragments at 58 ± 2 °C, which is the temperature of degradation, is expected to make crystalline ordered arrangements adding to the overall crystallinity. The % crystallinity, as reported (Table S2, Supporting Information), is calculated based
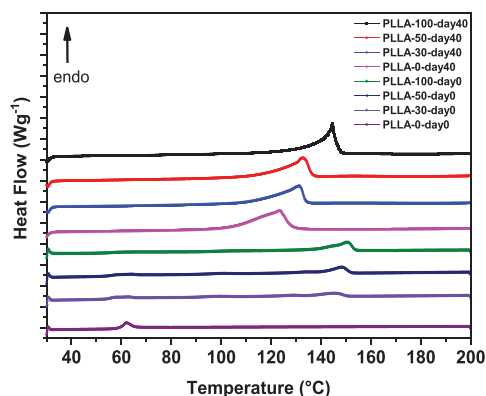
on the theoretical value of 93 J g^{-1} for 100% crystalline PLLA, assuming crystallization of PLLA is responsible for crystallinity in degraded blends also. Interestingly, the originally amorphous PLLA-0, which showed only a glass transition temperature (T_g) at 57 °C before degradation without any melting peak, presented an additional endothermic peak at 123 °C after undergoing a degradation process in the compost for 40 days. L- and D-rich segments after random cleavage of amorphous PLLA-0 could form a stereo-complex with racemic crystallites showing the melting peak at 123 °C. Although the high molar mass optically pure racemic crystallites show a melting peak at high temperature (210–240 °C), decreased melting point (140–180 °C) for the low molar mass stereo-complex is known.[25,26] The % crystallinity (X_c) for PLLA-0 is calculated based on the melting enthalpy of 142 J g^{-1} for stereo-complex crystals (Figure 7).[27] The stereo-complexes, and semi-crystalline leftover fractions are expected to degrade further but slowly, as known for the hydrolysis of stereo-complexes and highly crystalline polymers.[28]

After collecting and analyzing the undegraded samples in the compost test, the rest of the compost was extracted with chloroform with an aim to collect smaller undegraded fragments invisible to the naked eye, if any in solution for further analysis. The CO_2 evolution data as a measure of biodegradation, in this case, were not reliable due to interference from the gas evolving from composting of other organics in the compost.

Structural characterization of compost extract by ^{1}H-NMR shows similar peaks in the extract of test compost as that in the blank compost implying no significant degradation products in the compost, which could be extracted by chloroform (**Figure 8**).

An additional experiment was carried out by keeping PLLA-100 and PLLA-0 at 58 °C with high humidity for 50 days without compost in an oven for 100 days. In fact, the samples showed fragmentation to different molar mass fragments with very high crystallinity (Figure S6, Supporting Information, and corresponding data Table S2, Supporting Information). The PLLA-0 sample, which was otherwise amorphous, showed a melting peak at 97 °C after degradation, although the endothermic peak temperature is lower than that observed during composting. The % crystallinity (X_c) calculated is 56%. Interestingly, in GPC, several molar mass fractions, including very high molar masses, were also observed (Figure S7, Supporting Information). This is in contrast to the ones observed during actual degradation tests in the compost. This implies a complex degradation process occurring in compost with different degradation mechanisms leading to efficient degradation as compared to thermal degradation.

A biodegradation study was also performed in waste water collected from a local waste-water plant in a respirometer according to ISO 14851 for 38 days. The cumulative evolution of CO_2 was followed to judge the capability of samples to undergo biodegradation. **Figure 9** shows extremely slow biodegradation. Therefore, PLLA and its blends are not suitable for application where biodegradation in waste water is expected. Further, biodegradation tests in fresh water and artificial seawater for almost 1 year were carried out (Figure S8, Supporting Information). The various water types were characterized for the presence of biological activity by taxonomic classification analysis of the water system before starting the test (Figures S9 and S10, Supporting Information). No signs of degradation were observed in the freshwater,

ADVANCED
SCIENCE NEWS
www.advancedsciencenews.com

M acro-molecular
Materials and **Engineering**
www.mame-journal.de

Thermal properties			
Sample name	T_g [°C]	T_m [°C]	X_c [%]
PLLA-100-day40	45	143	86
PLLA-50-day40	44	132	72 (47)*
PLLA-30-day40	42	131	70 (46)*
PLLA-0-day40	44	123	56*
PLLA-100-day0	59	150	25
PLLA-50-day0	58	148	18
PLLA-30-day0	57	146	13
PLLA-0-day0	57	n.d.	0

Figure 7. DSC curves for PLLA and its blends with PDLLA before and after degradation in compost (left) and the corresponding data (right side). *X_c was calculated using melting enthalpy of 142 J g^{-1} for stereo-complex crystals. Melting temperature (T_m) was determined from the first heating cycle using DSC (scanning rate 10 K min^{-1} under nitrogen) except glass transition temperature (T_g), which was determined from second heating cycle.
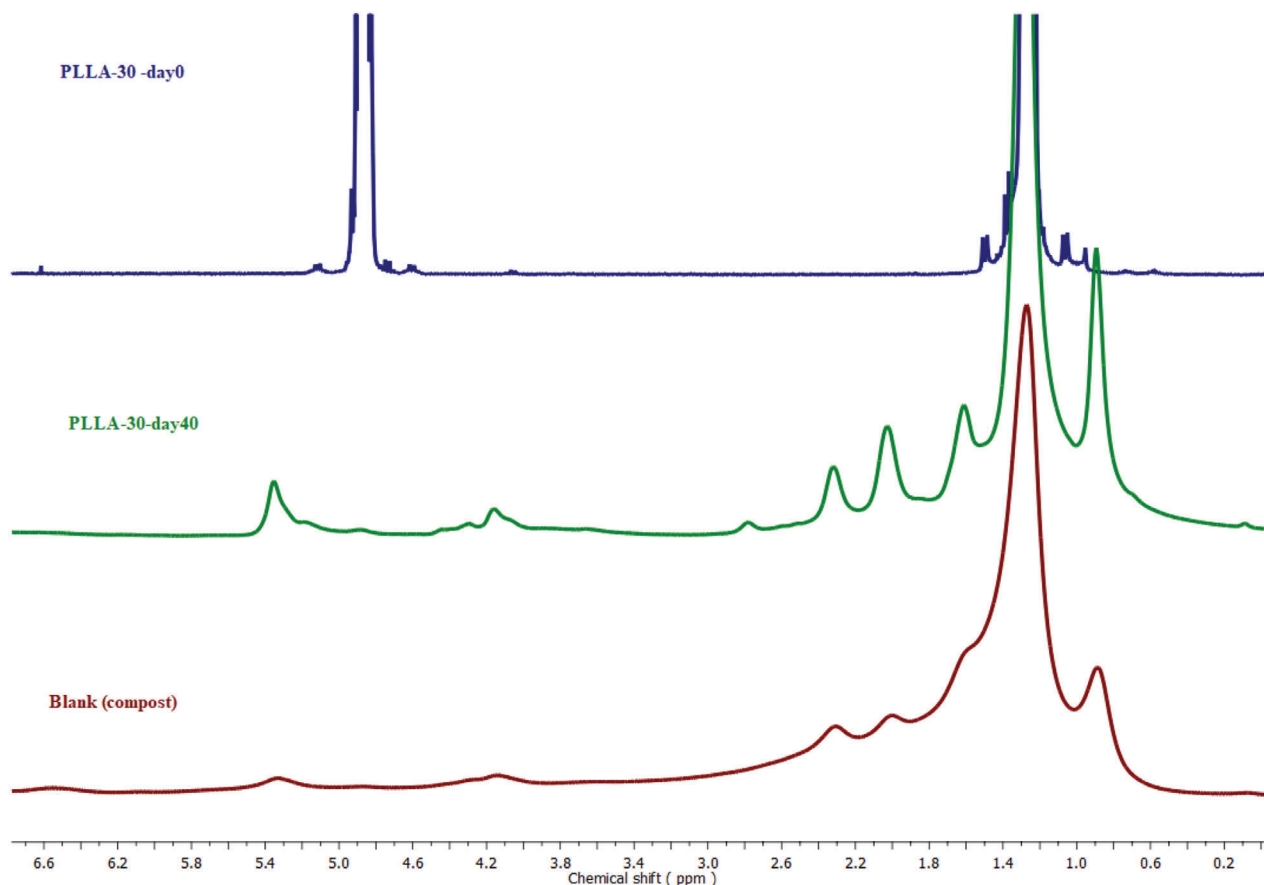

Figure 8. Comparison of Proton NMR for PLLA-30 in CDCl$_3$.

aquarium, and artificial seawater from weight loss data at least in 1-year period.

3. Conclusion

The physical characteristics and degradation behavior of blends of amorphous PDLLA with semi-crystalline PLLA prepared by solution casting were studied. The amorphous PDLLA did not disturb the crystallization of PLLA in blends. Therefore, blends were also semi-crystalline, unlike amorphous PDLLA but with reduced crystallinity. This was found to be highly optimum for balancing the mechanical properties with degradability. The blends were stronger in tensile testing in comparison to PDLLA with faster degradation. The blends showed degradation in compost
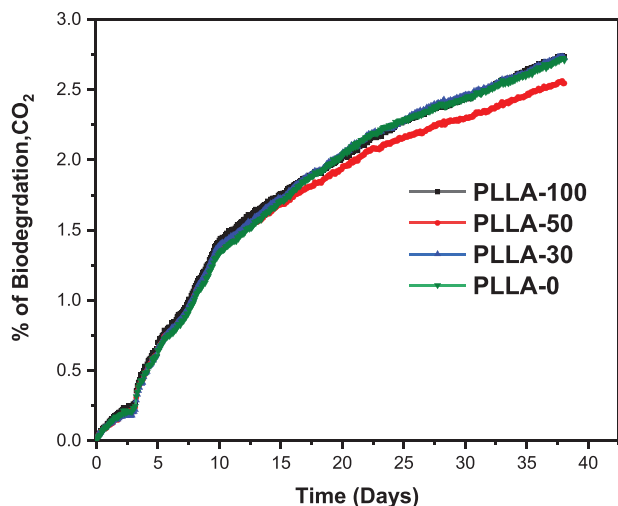
ADVANCED
SCIENCE NEWS
www.advancedsciencenews.com

[M] acro-
molecular
Materials and Engineering
www.mame-journal.de

Figure 9. Calculated percentage of biodegradation from CO_2 produced after 38 days according to the method in ISO 14851:2019.

by bulk degradation mechanism with the majority of degraded fractions in the very low molar mass region. Since there was an increase in the crystallinity of the rest of the undegraded samples in the compost after 40 days and even the formation of the stereo-complex is suspected, future studies are required with an extended degradation time period to understand the dynamic degradation behavior in compost. Their extremely slow degradation either in wastewater or other water bodies (fresh and seawater) exclude their use for applications expecting degradation in such environments. On the other hand, the blends come out as promising candidates for degradability in compost. Therefore, they will be studied in the future for compostable food packaging with appropriate modifications for gas permeability.

4. Experimental Section

Materials: The polylactide used in this work was the Ingeo 4043D grade semi-crystalline (PLLA), and Ingeo 4060D grade amorphous polymer (PDLLA) supplied by Nature Works, USA. Geneon GmBH, Germany, supplied proteinase K from fungus *Engyodontium album*. The activity was >30 units/mg and used as received. Chloroform (stabilized with 0.6% ethanol, VWR International), and Tris 1 м buffer solution, pH 9.0 were purchased from supplier abcr GmbH, Germany. Sodium azide (NaN_3) was used as received.

Preparation of Films: PLLA/PDLLA blends were prepared by mixing different percentages (100/0, 30/70, 50/50, 30/70, and 0/100, respectively) of a 3.3% w/w solution of PLLA and PDLLA in chloroform. PLLA/PDLLA solutions were poured into a glass petri dish with a diameter of 15 cm, and the film was dried first at room temperature for 24 h and then at a high vacuum at 70 °C for 3 days. The obtained films had a thickness of 170 ± 20 μm.

Enzymatic Degradation Test: The method used was as follows that was previously reported.[21] The authors reported here their results with the following modifications: films (2 cm × 1 cm) with thickness 170 ± 20 μm and weight of about 40 mg of each specimen were used. The films were incubated at 37 °C in 0.05 м Tris buffer solution (pH = 8.6 and 5 mL) having 0.025 mg mL⁻¹ of proteinase K together with 0.2 mg mL⁻¹ of NaN_3. The degradation medium was renewed every 24 h. The measurements were

done in triplicate. At definite time intervals, the undegraded samples were taken out or centrifuged for separation from solution depending upon the degree of degradation, and vacuum dried at room temperature for 1 week before further characterization. Blank runs were also carried out by incubating films in Tris buffer without any enzyme.

Compostability Test: Compostability test under laboratory conditions was performed under aerobic conditions. 4-week old compost was collected from the local compost unit, Buchestein, Bayreuth, and compost was sieved through 10 mm mesh before use. Samples with an average mass of 500 mg with the size of 1×1 cm² film pieces were placed in 175 g of compost at a humidity of 55–60% and then incubated in a water bath at a temperature of 58 ± 2 °C for 40 days.

Biodegradation Test: Films were tested in triplicate for ultimate biodegradation under aerobic conditions for 38 days. The testing methodology was based on DIN ISO 14851:2019. Activated sludge (at the end of nitrification) from the wastewater treatment plant at Bayreuth, Germany, was used as an inoculum. Approximately 75 mg of the film was added in 95 mL of standard medium and 5 mL of supernatant of activated sludge. Aniline was used as the positive sample. Activated sludge (without any organic substrate) in the same concentration was used as a control. The Micro-Oxymax respirometer equipped with a paramagnetic oxygen sensor and CO_2 sensor (Columbus Instruments International, USA) was used for the measurements.

Percentage of biodegradation was calculated by monitoring the production of CO_2 using Equation (1)

% of Biodegradation

$$= \frac{(mgCO_2 \text{ produced})_T - (mgCO_2 \text{ produced})_B}{ThCO_2} \times 100 \qquad (1)$$

where $(mgCO_2 \text{ produced})_T$ was the amount of CO_2 (in milligrams) that evolved from the Test material, $(mgCO_2 \text{ produced})_B$ was the amount of CO_2 (in milligrams) evolved in a control flask, and $ThCO_2$ was the theoretical amount of CO_2 that should be evolved from the test material, expressed in milligrams.

Methods: For the transparency test, samples were cut into a rectangular piece, placed directly in a UV–vis spectrophotometer test cell (Model V-630, Jasco spectrophotometer). Test samples (about thickness 170 μm) were measured using UV/vis spectrophotometer by measuring transmission at $\lambda = 650$ nm.

TGA were done with a Netzsch TG 209 F1 Libra under a nitrogen atmosphere. The heating rate of 10 K min⁻¹ and sample weight of about 5–10 mg were used for each measurement.

DSC was performed with a (Mettler Toledo DSC 2 STARe system) with a heating rate of 10 K min⁻¹ under a nitrogen atmosphere. The first heating cycle was used to determine melting peaks (T_m), and the second heating cycle was used to determine glass transition (T_g).

Crystallinity, X_c, was calculated from DSC using the following Equation (2):

$$X_c = \frac{\Delta H_f - \Delta H_{cc}}{\Delta H_f^\circ} \times 100\% \qquad (2)$$

ΔH_f was the observed enthalpy of fusion obtained from the first heating cycle of DSC measurement. ΔH_{cc} was the enthalpy of crystallization, ΔH_f° was the enthalpy of fusion of the completely crystalline PLLA. Here, ΔH_f° was 93 J g⁻¹ for PLLA.[20]

For CHCl₃-GPC analyses, an Agilent 1200 system equipped with a SDV precolumn (particle size 5 μm; PSS Mainz), a SDV linear XL column (particle size 5 μm, PSS Mainz), and a refractive index detector (Agilent Technologies 1260 Infinity) was used. Toluene (HPLC grade) was used as internal standard, and CHCl₃ (HPLC grade) was used as solvent at a flow rate of 0.5 mL min⁻¹ at room temperature. Calibration was based on narrowly distributed PS standards.

HFIP-GPC was conducted with an Agilent 1200 system equipped with a SDV precolumn (particle size 7 µm; PSS Mainz), a SDV linear XL column (particle size 7 µm, PSS Mainz), and a refractive index detector (Gynotek SE-61, Agilent Technologies). Toluene (HPLC grade) was used as an internal standard. Calibration was done with narrowly distributed PMMA standards from the company PSS Mainz. HFIP with potassium trifluoroacetate was used as solvent at a flow rate of 0.5 mL min^{-1} at room temperature.

For mechanical property testing, stress–strain tests were determined on a tensile instrument (Instron Universal Testing Machine 5565, Instron Engineering Corporation, USA). Tensile specimens were punched out (Coesfeld Material Test Inc., punching cutter, mold knife for tensile specimen DIN 53 504 S3A). The test was performed with crosshead speed 0.2 mm min^{-1} at room temperature and an average of ten measurements. The thickness of the specimens was measured with a digital micrometer.

SEM images were taken with a Zeiss LEO 1530 using an accelerating voltage of 3–10 kV.

Supporting Information

Supporting Information is available from the Wiley Online Library or from the author.

Acknowledgements

Conflict of Interest

The authors declare no conflict of interest.

Keywords

[1] J. M. Millican, S. Agarwal, *Macromolecules* **2021**, *54*, 4455.
[2] T. P. Haider, C. Völker, J. Kramm, K. Landfester, F. R. Wurm, *Angew. Chem., Int. Ed.* **2019**, *58*, 50.
[3] L. Filiciotto, G. Rothenberg, *ChemSusChem* **2021**, *14*, 56.
[4] S. Agarwal, *Macromol. Chem. Phys.* **2020**, *221*, 2000017.
[5] D. D. Harrier, P. J. A. Kenis, D. Guironnet, *Macromolecules* **2020**, *53*, 7767.
[6] S. H. Im, Y. Jung, S. H. Kim, *Macromolecules* **2018**, *51*, 6303.
[7] T. F. Burton, J. Pinaud, O. Giani, *Macromolecules* **2020**, *53*, 6598.
[8] P.-J. Roumanet, N. Jarroux, L. Goujard, J. Le Petit, Y. Raoul, V. Bennevault, P. Guégan, *ACS Sustainable Chem. Eng.* **2020**, *8*, 16853.
[9] V. Buchholz, S. Agarwal, A. Greiner, *Macromol. Biosci.* **2016**, *16*, 207.
[10] M. S. Reeve, S. P. Mccarthy, M. J. Downey, R. A. Gross, *Macromolecules* **1994**, *27*, 825.
[11] H. Tsuji, Y. Ikada, *J. Appl. Polym. Sci.* **1997**, *63*, 855.
[12] S. M. Li, H. Garreau, M. Vert, *J. Mater. Sci.: Mater. Med.* **1990**, *1*, 131.
[13] A. R. Bagheri, C. Laforsch, A. Greiner, S. Agarwal, *Global Challenges* **2017**, *1*, 1700048.
[14] J. Zhu, C. Habel, T. Schilling, A. Greiner, J. Breu, S. Agarwal, *Macromol. Mater. Eng.* **2019**, *304*, 1800779.
[15] H. Tsuji, Y. Ikada, *J. Appl. Polym. Sci.* **1996**, *60*, 2367.
[16] K. Fukushima, J. L. Feijoo, M.-C. Yang, *Polym. Degrad. Stab.* **2012**, *97*, 2347.
[17] Z. Ma, N. Zhao, C. Xiong, *Bull. Mater. Sci.* **2012**, *35*, 575.
[18] H. Tsuji, Y. Ikada, *J. Appl. Polym. Sci.* **1995**, *58*, 1793.
[19] S. Sato, D. Gondo, T. Wada, S. Kanehashi, K. Nagai, *J. Appl. Polym. Sci.* **2013**, *129*, 1607.
[20] L. Segal, J. J. Creely, A. E. Martin, C. M. Conrad, *Text. Res. J.* **1959**, *29*, 786.
[21] S. Li, A. Girard, H. Garreau, M. Vert, *Polym. Degrad. Stab.* **2000**, *71*, 61.
[22] W. Dong, B. Zou, Y. Yan, P. Ma, M. Chen, *Int. J. Mol. Sci.* **2013**, *14*, 20189.
[23] H. Tsuji, Y. Ikada, *J. Polym. Sci., Part A: Polym. Chem.* **1998**, *36*, 59.
[24] D. Cam, S.-H. Hyon, Y. Ikada, *Biomaterials* **1995**, *16*, 833.
[25] H. Tsuji, Y. Ikada, *Macromolecules* **1992**, *25*, 5719.
[26] S. Li, M. Vert, *Polym. Int.* **1994**, *33*, 37.
[27] E. W. Fischer, H. J. Sterzel, G. Wegner, *Kolloid Z. Z. Polym.* **1973**, *251*, 980.
[28] H. Tsuji, *Biomaterials* **2003**, *24*, 537.